Spatial Distribution of Trapped Calcite Particles in a Paul Trap: Measurement and Analysis

Matan Mahlev, Oren Gercenshtein, Shiran Eyal

The Hebrew University of Jerusalem, 3rd Year Physics Lab, January 2023

This study investigates the spatial distribution of calcite particles trapped in a Paul trap as a function of the applied voltage. The Paul trap is a commonly used device for trapping and manipulating small particles and has been shown to be effective for trapping calcite particles. In this experiment, calcite particles were trapped in the Paul trap and their spatial distribution was recorded and analyzed using image processing techniques. The results of the study show that the spatial variance of the trapped calcite particles decreases with increasing applied AC voltage. These findings have important implications for the manipulation and control of small particles using Paul traps, and may have applications in fields such as materials science, biotechnology, and quantum computing.

1. Introduction

Paul traps are devices that use oscillating electric fields to confine ions in a small region of space. They have been widely used in precision metrology, quantum computing, and other fields that require the manipulation of charged particles. The design of a Paul trap typically consists of a set of electrodes that create a quadrupole electric field, which is used to trap ions along the trap's central axis. The stability of the trapped ions depends on the amplitude and frequency of the trapping fields, as well as the properties of the trapped particles.

2. Theoretical Foundation

2.1 Earnshaw's Theorem

Earnshaw's theorem states that it is not possible to stably trap an electric charge using only the force of static electric or magnetic fields. This means that any attempt to confine a charged particle using only electrostatic or magnetostatic forces will ultimately fail. The proof of Earnshaw's theorem relies on the fact that a static electric or magnetic field can be represented as the gradient of a scalar potential function. For a stable equilibrium to exist, the force on a charged particle must be zero in all directions. However, the force on a charged particle in a static electric field is given by the negative gradient of the potential function. Since the gradient of a scalar potential is a vector, it cannot be zero in all directions unless the potential is constant. But this would mean that the electric or magnetic field is zero, which is not possible for a stable trapping configuration! Therefore, it is not possible to stably trap a charged particle using only static electric or magnetic fields.

2.1 Paul Trap – Simple Case

To overcome the above restriction, the Paul trap was introduced; Particles are elastically bound to an axis or a coordinate in space if a binding force acts on it which increases linearly with their distance r:

(Eq. 2.1) $$F(r) = -\alpha r$$

In other words, they move under a parabolic potential:

(Eq. 2.2) $$\phi \sim \alpha x^2 + \beta y^2 + \gamma z^2$$

Generally, if m is the number of 'poles' (as in monopole, dipole, etc.) or the order of symmetry, the potential is given by:

(Eq. 2.3) $$\phi \sim r^{\frac{m}{2}} \cos\left(\frac{m}{2}\varphi\right)$$

Where φ is angle of the direction of the setup. So, a general potential that suits the above conditions takes the form of:

(Eq. 2.4) $$\phi \sim \frac{\phi_0}{2r_0^2}(\alpha x^2 + \beta y^2 + \gamma z^2)$$

The Laplace condition $\Delta\phi = 0$ that must be obeyed, imposes:

(Eq. 2.5) $$\alpha + \beta + \gamma = 0$$

Which can be satisfied **simply** with a 2D configuration, or with a 3D configuration which contains cylindrical symmetry, making it easier to express in cylindrical coordinates:

(Eq. 2.6) $\phi = \frac{\phi_0(r^2-2z^2)}{r_0^2+2z_0^2}$ with $2z_0^2 = r_0^2$

Where $z_0 \equiv \sqrt{\left(z^2 - \frac{r^2}{2}\right)}$. The cylindrical symmetry of the above potential compels the shape of such trap to be hyperbolic.

A 'Paul trap' consists of 3 electrodes – a ring electrode and 2 end caps (see figure 2.1). The ring electrode is kept at ground potential, while the end caps are biased by an AC voltage of amplitude V_{ac}, at frequency Ω. We obtain the potential distribution:

(Eq. 2.7) $\phi(z,r) = \frac{V_{dc}-V_{ac}\cos(\Omega t)}{4z_0^2}[2z^2 + (r_0^2 - r^2)]$

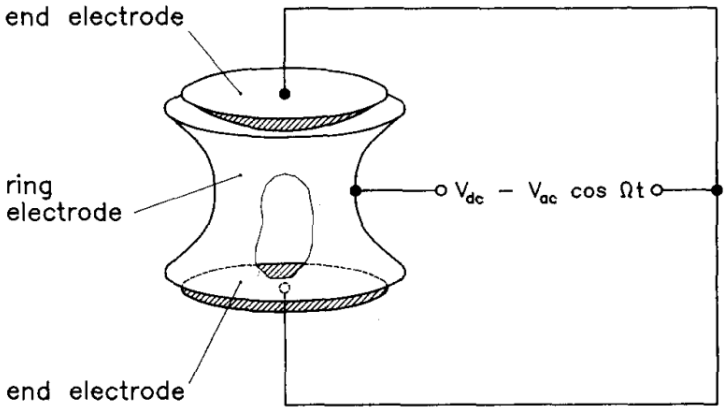

Figure 2.1 – A diagram of a Paul trap.

This potential implies electric field components that vary linearly with the coordinates:

(Eq. 2.8)

$$E_z = -\frac{\partial \phi}{\partial z} = -\frac{V_{dc} - V_{ac}\cos(\Omega t)}{z_0^2} z$$

$$E_r = -\frac{\partial \phi}{\partial r} = -\frac{V_{dc} - V_{ac}\cos(\Omega t)}{r_0^2} r$$

Resulting in the following equations of motion:

(Eq. 2.9)

$$\frac{d^2z}{dt^2} - \frac{Q}{M}\frac{V_{dc} - V_{ac}\cos(\Omega t)}{z_0^2} z = 0$$

$$\frac{d^2r}{dt^2} + \frac{Q}{M}\frac{V_{dc} - V_{ac}\cos(\Omega t)}{2z_0^2} r = 0$$

Where M is the particle mass, and Q its electric charge. The above equations of motions can be rewritten in the form of 'Mathieu differential equations':

(Eq. 2.10) $\frac{d^2u}{d\tau^2} + (a_u - 2q_u\cos(2\tau))u = 0$

Where:

- u represents the coordinate z or r
- τ is a unitless quantity which equals $\frac{\Omega t}{2}$
- *(Eq. 2.11)* $a_z = -2a_r \equiv 4\frac{Q}{M}\frac{V_{dc}}{z_0^2}\frac{1}{\Omega^2}$
- *(Eq. 2.12)* $q_z = -2q_r \equiv 2\frac{Q}{M}\frac{V_{ac}}{z_0^2}\frac{1}{\Omega^2}$

The parameter space for which there exist stable and unstable solutions for the Mathieu equations is shown in figure 2.2.

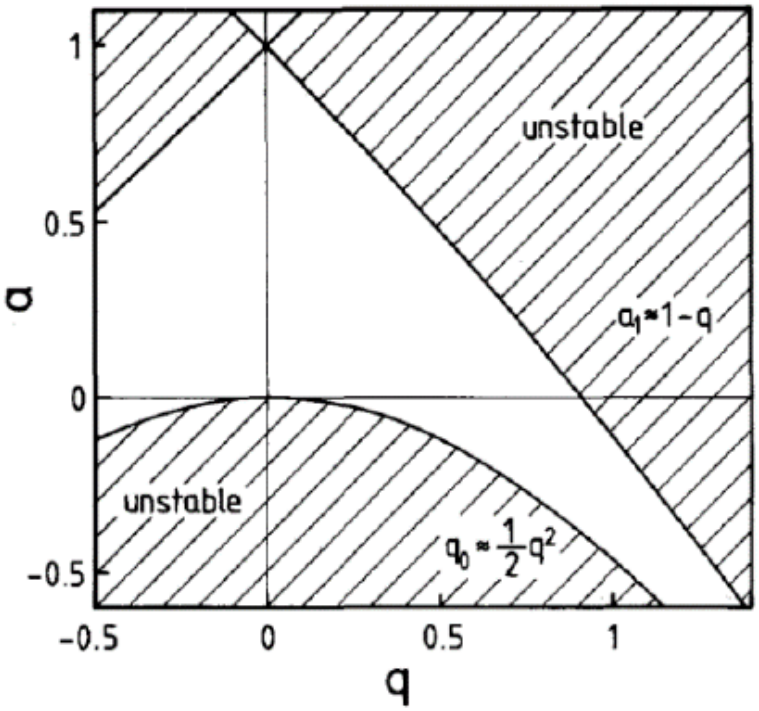

Figure 2.2 – The stability plot of Mathieu equation, in terms of parameters a, q. Displayed here is the close limit of these parameters, there exist other stable areas further away from the origin of this plot.

The area that we are interested in is the white area in Figure 2.2. To keep things as simple as possible, we determine the value of a to be 0 (which can be easily

achieved experimentally by introducing $V_{dc} = 0$). In this case, trapped particles must obey $q < 0.908$. From that we can immediately obtain an upper limit on the charge density of the particle from Eq. 2.12 -

(Eq. 2.13) $$\frac{Q}{M} < \frac{0.908}{2}\frac{z_0^2}{V_{ac}}\,\Omega^2$$

Concluding that in this case, the upper limit is inversely proportional to the magnitude of the AC voltage.

2.2 Approximate Solution, with Damping

Non-negligible damping in the system enlarges the size of the stability zone in the stability plot. In that case we assume the motion of the particle in the trap to be separated into two separate motions – an averaged secular motion $\bar{z}(t)$ and an oscillation $\delta(t)$ with frequency Ω:

(Eq. 2.14) $$z(t) = \delta(t) + \bar{z}(t)$$

Inserting the above relation into the Mathieu equations for the z-axis, whilst assuming $\delta \ll z$ and $\ddot{\delta} \gg \ddot{z}$, produces:

(Eq. 2.15) $$\frac{d^2z}{d\tau^2} \approx \frac{d^2z}{d\tau^2} = 2q_z\bar{z}(t)\cos(2\tau)$$

So that:

(Eq. 2.16) $$\delta(t) = -\frac{1}{2}q_z\bar{z}(t)\cos(\Omega t)$$

Now, taking the time-average over a period of the micromotion yields a differential equation for $\bar{z}(t)$:

(Eq. 2.17) $$\frac{d^2\bar{z}}{d\tau^2} = -\frac{q_z^2}{2}\bar{z}$$

Which results in:

(Eq. 2.18) $$\bar{z}(t) = \bar{z}_0\cos(\bar{\omega}_z t), \quad \bar{\omega}_z = \frac{q_z}{2\sqrt{2}}\Omega$$

2.3 Adding Gravity

Applying an external force F_z along the z axis (in case of gravity $F_z = Mg$) results in a biased variant of Eq. 2.17:

(Eq. 2.19) $$\frac{d^2\bar{z}}{d\tau^2} = -\frac{q_z^2}{2}\bar{z} + \frac{4g}{\Omega^2}$$

This causes a shift in position from the center of the trap, approximated by:

(Eq. 2.20) $$\Delta z_F = -\frac{8g}{\Omega^2 q_z^2} = -\frac{g}{\bar{\omega}_z^2}$$

Now, if we apply another force of $\frac{QV_z}{2z_0}$, along the positive direction of the z axis, we will receive:

(Eq. 2.21) $$\Delta z_F = -\frac{g}{\bar{\omega}_z^2} + \frac{QV_z}{2Mz_o\bar{\omega}_z^2}$$

And at the exact point where $\Delta z_F = 0$, the charge density of the particle is given by:

(Eq. 2.22) $$\frac{Q}{M} = \frac{2gz_0}{V_z}$$

2.4 Spatial Distribution of Confined Particles

As aforementioned, the Paul trap uses an alternating current (AC) voltage to confine charged particles in a small region of space. As the AC voltage is increased, the amplitude of the electric field also increases, and as a result, the trapping potential becomes stronger, and the confinement of the particles becomes tighter.

According to equation 2.21, we know that for a certain particle:

$$\Delta z_F \sim \frac{1}{\bar{w}_z^2} \sim \frac{1}{V_{ac}^2}$$

Therefore, we'll expect that each particle's average shift in the z-axis would decrease $\propto V_{ac}^2$. We thereby conclude:

(Eq. 2.23) $$STD[z] = \frac{\alpha}{V_{ac}^2}$$

Such that $$\alpha = \frac{1}{8}\left(\frac{M}{Q}\right)V_z * z_0^3 * \Omega^2\ [mm \cdot V^2]$$

Where the value for α was extracted from substituting the value for V_{ac}^2 taken from Eq. 2.12.

3. Experiment Setup

Our experimental system is very similar to the one described in chapter 2 (shown in figure 2.1), with a few minor differences; First, our end caps were connected to the V_{dc} and the ring electrode was connected to the V_{ac}. Second, our end caps were spherical, and not hyperbolic shaped, although they can be approximated to be hyperbolic from a close enough distance, which was the case in our experiment.

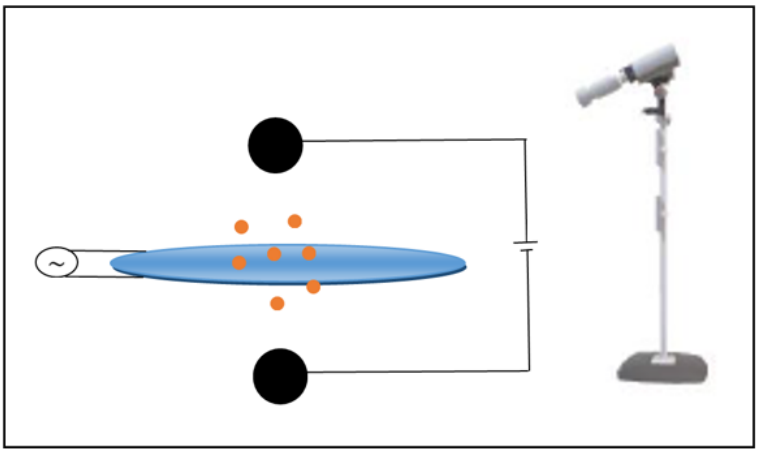

Figure 3.1 – A sketch of our experimental setup, for both parts of the experiment. Our setup is very much like Figure 2.1, with minor changes – the shape of the end electrodes is spherical (but from close ranges approximates a hyperbolic shape), the shape of the middle electrode is a ring. The brown dots stand for the confined particle cloud. On the right is an illustration of the high-fps camera we used for imaging.

3.1 Calibration

In the first part of the experiment, to make sure that our system is tuned, we filmed the particle under a constant AC voltage of 50 [Hz] frequency and checked to see if its movement in the z-direction is with a frequency of 50 [Hz]. We did that by applying a Fourier transform to its amplitude (in the z-direction) in time.

3.2 Charge Density

In the second part of the experiment, we applied a vertical voltage V_z in the range 2.95-10.57 [V] and measured the movement of the particle in the z-direction. Particularly, we measured its average z position, which is Δz_F in Eq. 2.21. We then fitted a linear curve, according to Eq. 2.21, whose slope should give us the charge-density $\frac{Q}{M}$.

3.3 Spatial Distribution of Confined Particles

In this part of the experiment, we began by trapping many particles using a large voltage (2.3 [kV]). Then for each value of V_{ac} we took a short video of the particles (0.5 [s], 120 [fps]). We slowly reduced V_{ac}, until most of the particles escaped the trap and repeated the measurement. Lowest voltage was 0.9 [kV]. Also, we kept V_{DC} constant at around -293 [V].

Using our data analysis methods, we extracted the average position of all the particles trapped and extracted the value of the standard deviation of these particles. We then constructed a plot of the results from which we extracted the charge density $\frac{Q}{M}$ once again.

3.4 Data Analysis

To analyze the data, whose nature was images obtained from a high-resolution camera, we used image processing techniques and Python scripting; For every video of a particle, for every image/frame of the video, the process was:

1. Clean the image from salt & pepper noise, using a 2D median filter.
2. Blur the image using a 2D Gaussian filter.
3. Crop only the relevant section (where the particles lie).
4. Position of the particles was found by applying a binary threshold filter of the mean pixel value (in the specific image).

This way we managed to extract the position of each of the particles for every frame of the video and analyze their spatial distribution.

4. Results

4.1 Calibration

Applying the Fourier transform for the z-movement of the particle indeed produced the correct driving AC voltage, as expected:

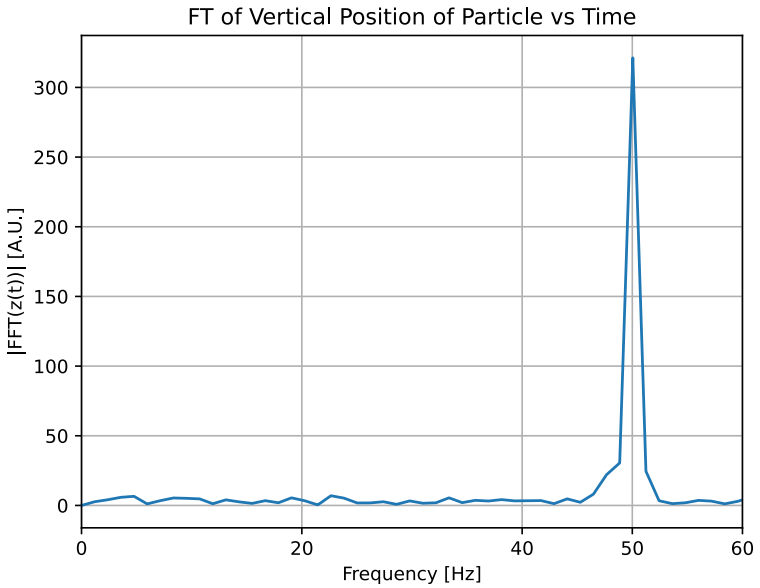

Figure 4.1 – Fourier transform of the movement of the particle in the z-direction. A clear peak can be seen where the frequency is 50 [Hz].

4.2 Charge Density

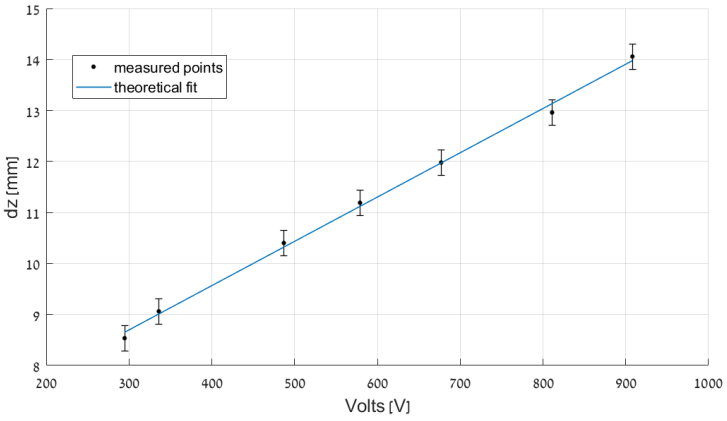

Figure 4.2 – The relation between height-difference (Δz_F) and the applied voltage (V_z). The graph is linear, with high statistical confidence ($R^2 = 0.99$). Errors were approximated using the Tracker program.

As shown in figure 4.2, the desired linear relation predicted by Eq. 2.21 was clearly seen. From the fit, the slope was numerically extracted, and using the values known in our system and plugging them into Eq. 2.21, a measured value of $\frac{Q}{M}$ was extracted:

$$\frac{Q}{M} = 7.8 \pm 0.9 * 10^{-4} \left[\frac{C}{kg}\right]$$

The expected values of charge density for calcite particles varies widely, depending on the size, composition, and environment of the particles. Calcite particles can reach up to a charge density of a few hundred $\left[\frac{\mu C}{Kg}\right]$ (see [1]), so our measured value is on the high end of the values but is indeed within range.

4.3 Spatial Distribution of Confined Particles

In this part we will examine the vertical spatial distribution on several particles as a function of V_{ac}. First, we present graphs of the spatial distribution of the particles for different values of V_{ac}:

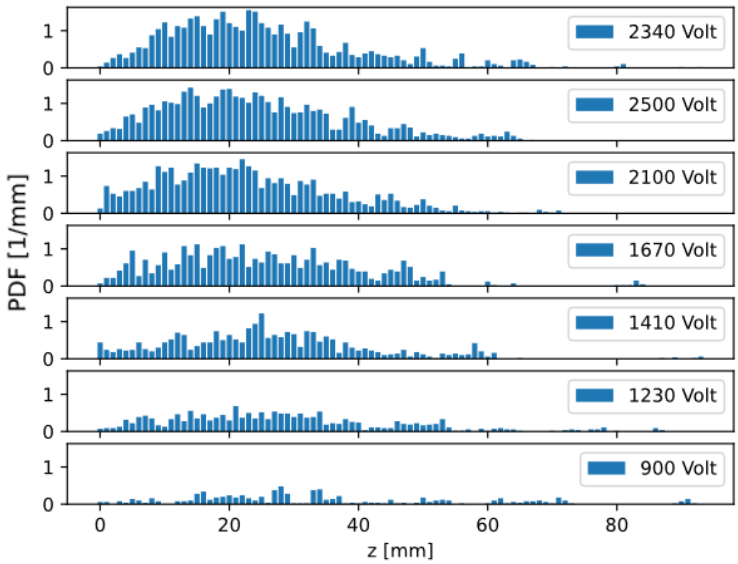

Figure 4.3 – Probability Density Function of the vertical position (z) of the particles. i.e., the average probability to find a particle at a specific z at any time.

From graph 4.3 we can clearly see the trend – at high voltages, the distribution is more concentrated about its average (z = 0, for calibration around the center of the trap). Its standard deviation (STD) is much smaller, and we can see a clearer gaussian shape.

At low voltages we see almost a uniform distribution, where the STD increases.

Next, we'll show a graph (Figure 4.4) of the standard deviation of distribution of the particles as a function of V_{ac}, along with a fit corresponding Eq. 2.2.

Examining Figure 4.4, we can clearly see the squared decrease of the standard deviation as a function of V_{ac}.

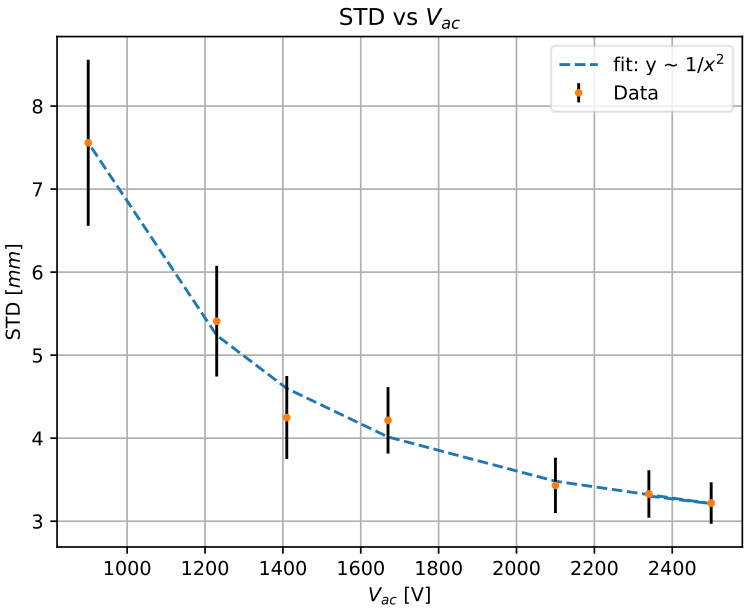

Figure 4.4 – Standard deviation of the vertical position (z) of the particles as a function of V_{ac}. Errors are approximated as constant, assuming 0.1 probability of double counting of particles. A fit (for $y = \frac{a}{x^2} + b$) was computed and the following parameters were extracted: $a = 4046 * 10^3 \pm 130 * 10^3$ $[mm \cdot V^2]$, $b = 2.56 \pm 0.2$ $[mm]$.

Using equation 3.3, inserting the values of the system along with the obtained value of the slope α, we get:

$$\frac{Q}{M} = (7.3 \pm 0.6) * 10^{-4} \left[\frac{C}{kg}\right]$$

Comparing this result to the result obtained in section 4.2, we receive significant statistical similarity between the two values, with:

$$N_\sigma = 0.91$$

Which means the values are less than a single standard-deviation from one another. However, we hypothesize that the small difference between the two results is because the latter represents the average value of Q/M over a set of particles, whereas in the section 4.2 we only examined one particle (which is also the reason for the difference in error estimation, which is larger for 1 particle in comparison to an average of several particles).

5. Discussion

Overall, our results are well within the accepted theoretical knowledge in the field: 1) A Fourier analysis of the particle movement yielded the correct input frequency. 2) Calculation of the charge density based on ΔZ_F gave us a value that sits well within a sensible range. 3) Variance of the spatial distribution of the particle-cloud yielded a very good statistical correlation with the desired equation (Eq. 2.23) and produced a charge-density value which is less than a single standard deviation away from the value we obtained beforehand.

One issue we encountered is that there exists no valuable information regarding the size and charge of the exact particles we used in this study. Therefore, all we could do is approximate whether our results were in a sensible range or not. Obtaining such values could be of great significance to the reliability of the results.

For future efforts in this field, we suggest experimenting with the particles' entropy in the trap, since entropy is one of the complementary measures to the variance that we calculated (entropy of the spatial distribution of the particles is closely related to their variance). The particles' frequency, kinetic energy, potential energy can be easily extracted and added to the calculation of entropy. Furthermore, we suggest approximating the theoretical Paul trap even more by:

1) Reducing the size of the system (practically reduces z_0) thus making our assumption that the spherical caps behave like the hyperbolic caps more accurate.

2) Finding a neat way to inject the trap with one particle at a time. This will reduce the data-analysis efforts, causing errors to shrink, thus producing more accurate results (of charge density for instance).

3) Finding an efficient way to confine many particles for each value of the voltages in the interesting range.

6. Appendices

1) All errors for the resulting values were calculated using a formula for error propagation:

$$\Delta = \sqrt{\sum \left(\frac{\partial f}{\partial x_i}\right)^2 \Delta x_i^2}$$

Where $f(x_i)$ is the value to be determined, and Δx_i^2 where wither previously known or determined by a smart guess.

2) An example of an image of the particle cloud taken from one of the images:

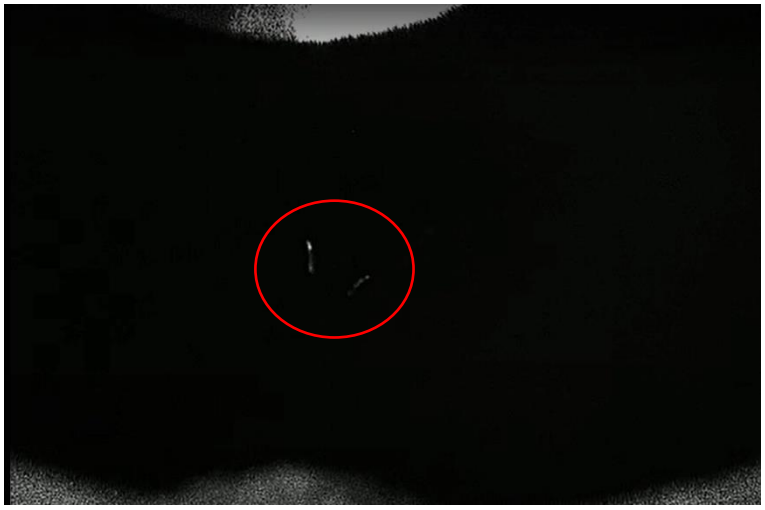

The particle cloud in the above image is circled in red.

7. Bibliography

1) J. B. Rundle, "Charge density of atmospheric dust particles", Journal of Geophysical Research, 1971.

2) H. Winter and H.W. Ortjohann, "Simple Demonstration of storing macroscopic particles in a Paul trap", University of Münster, 1990.

3) P. Wolfgang, “Electromagnetic traps for charged and neutral particles”, Bonn University, 1990.